Eur. Phys. J. C 29, 37–44 (2003)
Digital Object Identifier (DOI) 10.1140/epjc/s2003-01214-5

THE EUROPEAN PHYSICAL JOURNAL C

The QCD pomeron in ultraperipheral heavy ion collisions: II. Heavy quark production

V.P. Gonçalves[1,a], M.V.T. Machado[1,2,b]

[1] Instituto de Física e Matemática, Universidade Federal de Pelotas, Caixa Postal 354, CEP 96010-090, Pelotas, RS, Brazil
[2] High Energy Physics Phenomenology Group, IF-UFRGS, Caixa Postal 15051, CEP 91501-970, Porto Alegre, RS, Brazil

Received: 30 January 2003 / Revised version: 26 March 2003 /
Published online: 13 May 2003 –

Abstract. The heavy quark production in ultraperipheral heavy ion collisions is investigated, with particular emphasis on the results from the coherent interactions given by the two-photon process. One addresses the heavy quark total cross sections at photon level considering the saturation model and the BFKL dynamics in the color dipole picture. The corresponding cross sections at nuclear level are presented. It is verified that the QCD dynamics implies an enhancement of the cross section in comparison with previous calculations.

1 Introduction

The behavior of ep/pp scattering in the limit of high center-of-mass energy $\sqrt{s}$ and fixed momentum transfer is one of the outstanding open questions in the theory of the strong interactions. In the late 1970s, Lipatov and collaborators [1] established the papers which form the core of our knowledge of the Regge limit (high energy limit) of quantum chromodynamics (QCD). The physical effect that they describe is often referred to as the QCD pomeron, with the evolution described by the BFKL equation. The simplest process where this equation applies is the high energy scattering between two heavy quark–antiquark states, i.e. the onium–onium scattering. For a sufficiently heavy onium state, high energy scattering is a perturbative process since the onium radius gives the essential scale at which the running coupling $\alpha_{\rm s}$ is evaluated. This process was proposed as a gedanken experiment to investigate the high energy regime of QCD in [2–4] (see also [5]). In the dipole picture [2], the heavy quark–antiquark pair and the soft gluons in the limit of a large number of colors N_c are viewed as a collection of color dipoles. In this case, the cross section can be understood as a product of the number of dipoles in one onium state, the number of dipoles in the other onium state and the basic cross section for dipole–dipole scattering due to two-gluon exchange. At leading order (LO), the cross section grows rapidly with the energy ($\sigma \propto \alpha_{\rm s}^2\, {\rm e}^{(\alpha_{\rm I\!P}-1)Y}$, where $(\alpha_{\rm I\!P}-1) = \frac{4\alpha_{\rm s}\, N_c}{\pi}\, \ln 2$ and $Y = \ln s/Q^2$) because the number of dipoles in the light cone wave function grows rapidly with the energy. Therefore, in principle, the analysis of the energy dependence of the cross section could disentangle the QCD pomeron effects. However, for ep/pp colliders, the study of the QCD pomeron is made difficult by the fact that the cross section is influenced by both short and long distance physics. Only when specific conditions are satisfied is it that one can expect to determine the QCD pomeron effects. Some examples are the forward jet production in deeply inelastic events at low values of the Bjorken variable x in lepton–hadron scattering and jet production at large rapidity separations in hadron–hadron collisions.

Over the past few years much experimental effort has been devoted towards the observation of the QCD pomeron in those processes, but the conclusions are not unambiguous (see e.g. [6]). This fact is mainly associated with the theoretical uncertainty present in the high energy limit of QCD. Only recently, after an effort of ten years, the next-to-leading order (NLO) corrections to the BFKL equation were obtained (for a review on NLO BFKL corrections, see e.g. [7] and references therein). Moreover, since the BFKL equation predicts that for $s \to \infty$ the corresponding cross section rises with a power law of the energy, violating the Froissart bound, new dynamical effects associated with the unitarity corrections are expected to stop further growth of the cross sections [8]. This expectation can be easily understood: while for large transverse momentum $k_\perp$, the BFKL equation predicts that the mechanism $g \to gg$ populates the transverse space with a large number of small size gluons per unit of rapidity (the transverse size a gluon with momentum $k_\perp$ is proportional to $1/k_\perp^2$), for small $k_\perp$ the produced gluons overlap and fusion processes, $gg \to g$, are equally important. Considering this process, the rise of the gluon distribution with transverse momenta below a typical scale, which is energy dependent, called the saturation scale $Q_{\rm s}$,

[a] e-mail: barros@ufpel.tche.br
[b] e-mail: magnus@if.ufrgs.br

is reduced, restoring the unitarity. It is important to point out the salient fact that Golec-Biernat and Wusthoff [9] have shown that a saturation model is able to describe the DESY *ep* collider HERA data, in particular the transition from the perturbative to the non-perturbative photoproduction region, including the inclusive and diffractive cross sections. Therefore, the description of the QCD pomeron still is an open question, which deserves a more detailed analysis.

This situation should be improved in the future with the next generation of linear colliders. (For a recent review of BFKL searches, see e.g. [6].) In particular, future e^+e^- colliders probably will allow one to discriminate between BFKL and saturation predictions [10] (For another analysis of photon–photon collisions, see [11–13]). Such a reaction presents analogies with the process of scattering of two onia discussed above. Although the onium–onium scattering is a gedanken experiment, off-shell photon scattering at high energy in $e^+\,e^-$ colliders, where the photons are produced from the lepton beams by bremsstrahlung, plays a similar role. In these two-photon reactions, the photon virtualities can be made large enough to ensure the applicability of the perturbative methods. Similarly, we can expect that we can test the QCD pomeron in heavy flavor production in two-photon collisions, where the hard scale is provided by the heavy quark mass.

In the last years many authors have studied in detail the process referred to. From the point of view of the color dipole picture, in [10] the contribution of the dipole–dipole interaction was taken into account considering a generalization of the original saturation model [9] to the two-photon reactions. There, the results present good agreement with the data from e^+e^- colliders, there remaining some room to discuss issues concerning resolved contributions. In [14], these questions were revisited using the saturation model, where threshold effects were addressed in an accurate way as well as that the hadronic single resolved contribution was computed within the dipole formalism. A current open question is the discrepancy between the theoretical results and the data on heavy quark production, mostly for the bottom case, in the γp photoproduction and two-photon reactions. This feature is also corroborated by the dipole–dipole approach from [15]. As found in [14], even the inclusion of resolved contributions does not remove completely the observed deficit. Quite promising results are obtained in [16], where heavy quark production in the two-photon reaction is calculated within the $k_\perp$-factorization formalism and the unintegrated gluon density for the photon is determined using the saturation model.

From the point of view of the BFKL approach, there are several calculations using the leading logarithmic approximation [11–13] and considering the next-to-leading corrections to the total cross section $\gamma^*\gamma^*$ process [13,17]. In particular, a stable next-to-leading order program relying on the BLM optimal scale setting [19] has produced good results with OPAL and L3 data at LEP2 [17]. However, the heavy quark production from a real two-photon process is still an open question. Only the effects of the charm mass in the $\gamma^*\gamma^*$ total cross section for the kinematical region of L3 at LEP was analyzed by Bartels et al. [18] considering the LO BFKL dynamics. We address that issue in our analysis, considering a BFKL dipole approximation to the QCD dynamics. Similarly to the previous analysis on two-photon physics, one shows that the next generation of colliders will be able to discriminate the dynamics associated to the QCD pomeron.

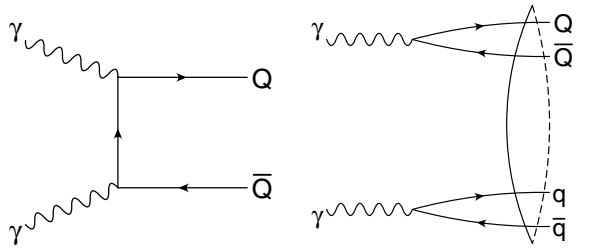

Fig. 1. The diagrams contributing to the QPM piece (*left panel*) and dipole–dipole interactions (*right panel*). Figures are from [10]

Recently, we have proposed in [20] to investigate QCD pomeron effects in a different context, namely in photon–photon scattering at ultraperipheral heavy ion collisions. In this case, the cross sections are enhanced since the $\gamma\gamma$ luminosity increases as Z^4, where Z is the atomic number [21,22]. There we have analyzed the double diffractive J/Ψ production in $\gamma\gamma$ collisions, with the photons coming from the Weizsäcker–Williams spectrum of the nuclei. For that process our results have indicated that a future experimental analysis can be useful to discriminate the QCD dynamics at high energies. Here we extend our proposal for heavy quark production. In principle, at ultraperipheral heavy ion collisions, a photon stemming from the electromagnetic field of one of the two colliding nuclei can interact with one photon of the other nucleus (two-photon process) or can penetrate into the other nucleus and interact with its hadrons (photon–nucleus process). Therefore, heavy quarks can be produced in photon–nucleus interactions as well as photon–photon interactions. The first case has been extensively discussed in the literature [23–25] (for a review, see [26]) and recently revised in different approaches [27–29]. On the other hand, heavy quark production in two-photon collisions has been discussed essentially in [29–31]. In these analyses, the underlying contribution comes from the QED quark-box diagram (QPM) at LO [Fig. 1 (left panel)], which dominates in the available energies at RHIC, $W_{\gamma\gamma} \leq 6\,\mathrm{GeV}$. In [29], besides the direct contribution also the resolved contributions were carefully calculated and the latter is shown to be negligible. However, at the LHC experiment, where the two-photon energies can reach $W_{\gamma\gamma} \leq 200\,\mathrm{GeV}$, the QCD diagrams become important and the QCD pomeron should dominate in this limit [Fig. 1 (right panel)]. Consequently, an enhancement of the cross section associated to the dynamics is expected. We will address these issues in Sect. 3, complementing the detailed study presented in [29].

Here, we will restrict our analysis to the two-photon process and its potentiality to investigate the QCD dy-

namics. Similarly as in [20], our goal here is twofold: to analyze the potentiality of this process to constrain the QCD dynamics at high values of energy and to provide reliable estimates for the cross sections concerning that reaction. Relativistic heavy ion collisions are a potentially prolific source of $\gamma\gamma$ collisions at high energy colliders. The advantage of using heavy ions is that the cross sections varies as $Z^4\alpha^4$, rather than only α^4. Moreover, the maximum $\gamma\gamma$ collision energy $W_{\gamma\gamma}$ is $2\gamma/R_A$, about 6 GeV at RHIC and 200 GeV at LHC, where R_A is the nuclear radius and γ is the center-of-mass system Lorentz factor of each ion. For two-photon collisions, the cross section for the reaction $AA \to AAQ\overline{Q}$, where $Q = c$, b, will be given by

$$\sigma_{AA\to AA\,Q\overline{Q}}\,(s) = \int \mathrm{d}\tau\, \frac{\mathrm{d}\mathcal{L}_{\gamma\gamma}}{\mathrm{d}\tau}\, \hat{\sigma}_{\gamma\gamma\to Q\overline{Q}}\,(\hat{s}), \qquad (1)$$

where $\tau = \hat{s}/s$, $\hat{s} = W^2_{\gamma\gamma}$ is the square of the center-of-mass (c.m.s.) system energy of the two photons, s of the ion–ion system, $\mathrm{d}\mathcal{L}_{\gamma\gamma}/\mathrm{d}\tau$ is the photon luminosity, and $\hat{\sigma}_{\gamma\gamma\to Q\overline{Q}}(\hat{s})$ is the cross section of the $\gamma\gamma$ interaction (for details related to the numerical expressions, see [20]). Our approach excludes possible final state interactions of the produced particles with the colliding particles, allowing reliable calculations of the ultraperipheral heavy ion collisions. Therefore, to estimate the heavy quark production it is only necessary to consider a suitable QCD model for the photon–photon interaction.

This paper is organized as follows. In Sect. 2, we calculate the total cross sections for the process $\gamma\gamma \to Q\bar{Q}$ based on the color dipole picture, using the dipole cross section given by the saturation model and BFKL approach. In Sect. 3, the corresponding heavy quark cross section in coherent ultraperipheral heavy ion collisions are presented, with a particular emphasis in the LHC energies. In the last section we draw our conclusions and summarize the main results.

2 Heavy-quark production at the photon level

Heavy quark production via photon–photon collisions is a powerful process testing the applicability of perturbative QCD methods. The photon induced reactions have the advantage of being clear concerning the probing structure, and the large mass of the heavy quarks produced allows perturbative physics to be employed. The production mechanisms of such processes have been systematically studied, despite the available data being modest and having large uncertainties (see [32] and references therein). An important experimental verification is that the data on open heavy quark pair production, mostly for the bottom quark, stay above the theoretical calculations by a sizable factor. Such a feature has generated several studies which rely on higher orders in the collinear factorization approach or on the successful results based on the semihard approach.

An important approach describing the two-photon process is given by the color dipole formalism [2,5]. The simple physical picture is provided by the photon splitting in a quark–antiquark pair (virtual components in the transverse plane), called a color dipole, long after the interaction and the further scattering of these pairs with the target. Such an approach has produced a consistent and unified description of high energy photon induced processes in deep inelastic scattering and two-photon reactions, including the deep inelastic diffractive dissociation. In particular, in the two-photon interactions, the target is also given by a color dipole. The wave functions describing the photon's virtual fluctuation are completely determined from perturbative methods, whereas the effective color dipole cross section has to be modelled. It may contain non-perturbative and higher twist contributions as well as parton saturation effects as we should discuss later on.

The $Q\bar{Q}$ pair production mechanism can be separated into three main contributions:

(i) the quark box diagram (QPM), with photons coupling to the same heavy quark line, which dominates at not so large photon–photon c.m.s. energies $W_{\gamma\gamma}$ [Fig. 1 (left panel)];

(ii) the dipole–dipole interaction, where both photons fluctuate in quark–antiquark pairs and interact through gluonic exchange, which dominates at high energies [Fig. 1 (right panel)];

(iii) single and double resolved contributions, where one of the photons fluctuates into the vector mesons (ρ, ω, ϕ, ...) interacting with the remaining dipole, being a background to the dipole–dipole reaction. The first contribution is well known, providing a $W^{-2}_{\gamma\gamma}$ behavior modulo logarithmic corrections, given by for example [33,34]. The second one will be reproduced in the following, making use of a sound model for the dipole cross section [10]. The third one will be disregarded, but we quote the study presented in [14], where these pieces were calculated for the first time in the color dipole approach.

The color dipole formulation gives the following expression for the heavy quark pair production in a (real) two-photon reactions at high energies:

$$\begin{aligned}
&\sigma^{\mathrm{dd}}(\gamma\gamma \to Q\bar{Q}) \\
&= \sum_{q_1\neq Q} \int |\Psi_{q_1\bar{q}_1}(\boldsymbol{r}_1, z_1)|^2\, |\Psi_{Q\bar{Q}}(\boldsymbol{r}_2, z_2)|^2\, \sigma_{\mathrm{dd}}\,(\boldsymbol{r}_1, \boldsymbol{r}_2, \tilde{x}_{ab}) \\
&\qquad \times \mathrm{d}^2\boldsymbol{r}_1\, \mathrm{d}^2\boldsymbol{r}_2\, \mathrm{d}z_1\, \mathrm{d}z_2 \\
&+ \sum_{q_2\neq Q} \int |\Psi_{Q\bar{Q}}(\boldsymbol{r}_1, z_1)|^2\, |\Psi_{q_2\bar{q}_2}(\boldsymbol{r}_2, z_2)|^2\, \sigma_{\mathrm{dd}}\,(\boldsymbol{r}_1, \boldsymbol{r}_2, \tilde{x}_{ab}) \\
&\qquad \times \mathrm{d}^2\boldsymbol{r}_1\, \mathrm{d}^2\boldsymbol{r}_2\, \mathrm{d}z_1\, \mathrm{d}z_2\,, \qquad (2)
\end{aligned}$$

where $\Psi_{q\bar{q},\,(Q\bar{Q})}(\boldsymbol{r}, z)$ are the light (heavy) quark–antiquark wave functions of the photon in the mixed representation. The transverse separation (dipole size) of the respective quark pair is denoted by $\boldsymbol{r}$ and their longitudinal momentum fraction denoted by z. The dipole–dipole cross section, σ^{dd}, depends on the dipole sizes and on the parameter $\tilde{x}_{ab}$, driving the energy behavior.

First, we write down the expressions for the wave functions squared including the respective quark helicities T, L and the photon virtuality defined as Q^2,

$$|\Psi_{\rm T}(\boldsymbol{r},z)|^2 = \frac{6\,\alpha_{\rm em}}{4\,\pi^2}\sum_f e_f^2\,[z^2+(1-z)^2]\,\varepsilon_f^2\,K_1^2\,(\varepsilon_f\,r) + m_f^2\,K_0^2\,(\varepsilon_f\,r)\,, \quad (3)$$

$$|\Psi_{\rm L}(\boldsymbol{r},z)|^2 = \frac{6\,\alpha_{\rm em}}{4\,\pi^2}\sum_f e_f^2\,4\,Q^2\,z^2(1-z)^2\,K_0^2\,(\varepsilon_f\,r)\,, \quad (4)$$

where e_f and m_f stand for the charge and mass of the quark having flavor f, and the $K_{0,1}$ are the McDonald–Bessel functions. The auxiliary variable ε is defined as $\varepsilon^2 = z(1-z)\,Q^2 + m_f^2$ which in the real photon case, $Q^2 = 0$, considered here, simplifies to $\varepsilon = m_f$. Also, in such a case, the longitudinal photon component is obviously suppressed. The light quark masses are considered to be equal and an effective value of $m_q \sim 0.2$ is determined from fitting the two-photon data [10].

Let us discuss now a specific model for the dipole–dipole cross section. Here, we follow the formulation of the saturation model applied to two-photon reactions [10]. The cross section describing the dipole interaction satisfies the saturation property, i.e. a constant dependence on the energy at large dipole sizes, and color transparency behavior at small dipole sizes. The interface between these two regions is controlled by the saturation scale, which is energy dependent and has been determined from fitting the data on small-x deep inelastic data [9]. Explicitly, the dipole–dipole cross section takes the eikonal-like form,

$$\sigma_{\rm dd}\,(\boldsymbol{r}_1,\boldsymbol{r}_2,\tilde{x}_{ab}) = \tilde{\sigma}_0\,\left[1-\exp\left(-\frac{\bar{r}^2}{4\,R_0^2\,(\tilde{x}_{ab})}\right)\right]\,, \quad (5)$$

with the overall normalization given by $\tilde{\sigma}_0 = (2/3)\,\sigma_0$ inspired by the quark-counting rule, and where σ_0 is determined for the proton case analysis in [9]. The effective radius $\bar{r}$ is constructed is such way as to reproduce the dipole–hadron parameterization, i.e. $\bar{r}^2 \sim \boldsymbol{r}_1^2\,(\sim \boldsymbol{r}_2^2)$ in the dipole configurations $\boldsymbol{r}_2^2 \gg \boldsymbol{r}_1^2$ ($\boldsymbol{r}_1^2 \gg \boldsymbol{r}_2^2$). Here, we will consider two possibilities giving good results as found in [10]:

(I) $\bar{r}^2 = r_1^2\,r_2^2/(r_1^2+r_2^2)$, preferable against the two-photon data;

(II) $\bar{r}^2 = \min(r_1^2,\,r_2^2)$, preferable for the charm quark pair production data.

The fitted mass for the light quarks takes the value $m_q = 0.21\,\text{GeV}$ considering the effective radius (I) and $m_q = 0.23\,\text{GeV}$ using radius (II). The saturation radius R_0 squared reads

$$R_0^2\,(\tilde{x}_{ab}) = \left(\frac{\tilde{x}_{ab}}{x_0}\right)^{\lambda}\,\text{GeV}^{-2}\,, \quad (6)$$

where the parameters x_0 and λ are also determined in the original saturation model in the proton case [9]. The saturation scale, $Q_{\rm s}(\tilde{x}_{ab})$, is obtained by the inverse of the saturation radius described above. The effective variable $\tilde{x}$ depends on the two-photon energy and the quark masses and reads

$$\tilde{x}_{ab} = \frac{4\,m_a^2 + 4\,m_b^2}{W^2}\,, \quad (7)$$

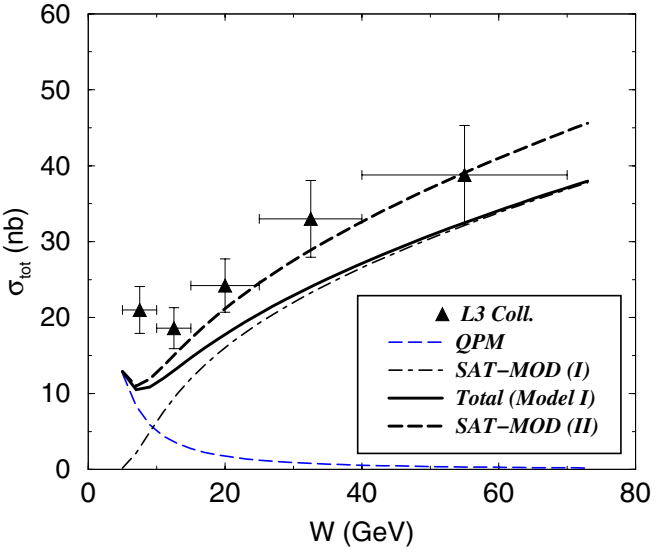

Fig. 2. The cross section for the inclusive charm production in two-photon reactions. The QPM contribution (*thin dashed line*) is shown separately. The saturation model considering different effective radii are represented by the solid (model I) and long-dashed (model II) curves. Data are from the L3 Collaboration

where in the heavy quark production a and b correspond to a light and a heavy (or vice versa) quark. For low energy (large $\tilde{x}$), the dipole cross section needs to be supplemented by threshold effects. Following [10], they are taken into account through the multiplicative factor $(1-\tilde{x}_{ab})^5$, coming from dimensional-counting rules. However, a different procedure is adopted in [14], where the threshold is considered by imposing the kinematical constraint $M_{q\bar{q}} + M_{Q\bar{Q}} < W_{\gamma\gamma}$ in the integrations at (2), where M is the invariant mass of the pair. There, also the variable $\tilde{x}$ takes a different form than (7), depending explicitly on z_1 and z_2.

In Fig. 2 we reproduce the results on charm production considering the saturation model (SAT-MOD), regarding the quark box contribution (QPM) and the dipole–dipole approach using the saturation model. The theoretical predictions are compared with the experimental results from the L3 Collaboration [35]. It should be stressed that results for the bottom case are straightforward, changing only the quark charge and mass, $e_b = 1/3$ and $m_b = 4.5\,\text{GeV}$. The charm mass is taken as $m_c = 1.3\,\text{GeV}$ and the two prescriptions for the effective radius are presented. The QPM contribution (long-dashed curve) is very important at low energy, starting to be negligible around $W_{\gamma\gamma} = 10\,\text{GeV}$. Therefore, this contribution should dominate the ultraperipheral heavy quark production at RHIC energies, where the maximal $W_{\gamma\gamma}$ reached is of order of a few GeV. However, above $W_{\gamma\gamma} \geq 10\,\text{GeV}$, the dipole–dipole approach dominates the physical description, providing an increase of the total cross section. The results using the effective radius (I) (solid line) and (II) (dashed line) are presented. The contribution from dipole–dipole interaction is shown separately for the radius (I), represented by the

dot-dashed line. This contribution plays a very important role at LHC energies, where the two-photon energy in ultraperipheral collisions can reach up to $W \sim 160\,\mathrm{GeV}$.

Regarding the resolved (single and double) contributions, we have not considered these here. We quote [14], where these contributions are calculated using the saturation model within the dipole–dipole picture. There it was found that for the charm case the single resolved piece constitutes about 30% of the main contribution. In the bottom case, these contributions are quite smaller.

A prominent challenge in high energy physics concerns the issue of what the correct dynamics is, driving the interaction at asymptotic energies. It is basically dominated by gluonic interactions and the saturation model discussed above successfully interpolates between the soft (non-perturbative) and hard (perturbative) regimes, whose transition relies on the parton saturation phenomenon. However, the physics of two-photon collisions is an optimal tool for testing the BFKL approach [1]. In its dipole formulation, the BFKL dynamics is suitable to describe the interaction of small size color dipoles from the interacting photons. A lot of work has been done using the LO BFKL approach and also attempts to include NLO corrections in two-photon reactions [11–13,17,18]. However, heavy quark production in real photon–photon collisions considering the BFKL approach was not addressed in the current literature. Below, we present our results for this case.

To estimate the heavy quark production in the BFKL approach we need a model for the dipole–dipole cross section. In particular, the BFKL dipole cross section can be obtained from the momentum representation and it can be considered as a solution of the linearized Balitsky–Kovchegov equation in the coordinate space [8,36]. The LO BFKL solution is completely known in the momentum space, providing a steep energy dependence associated with the hard pomeron intercept $1+\omega_{\mathbb{P}}$ and the typical diffusion feature. For our purpose here, we will consider the following expression for the dipole–dipole cross section from the BFKL dynamics:

$$\sigma_{\rm dd}\left(\boldsymbol{r}_1,\boldsymbol{r}_2,\tilde{x}_{ab}\right) = \frac{4\,\pi^2}{3}\,\mathcal{C}\,\left(\frac{\bar{r}^2}{\bar{r}_0^2}\right)^{\frac{1}{2}} \times \frac{\mathrm{e}^{\,\omega\,\bar{\alpha}_{\rm s}\,\ln(1/\tilde{x}_{ab})}}{\sqrt{2\,\pi\,\tilde{\omega}\,\bar{\alpha}_{\rm s}\,\ln(1/\tilde{x}_{ab})}}\,\exp\left[\frac{-\ln^2\left(\bar{r}^2/\bar{r}_0^2\right)}{2\,\tilde{\omega}\,\bar{\alpha}_{\rm s}\,\ln(1/\tilde{x}_{ab})}\right] \times \left(1-\tilde{x}_{ab}\right)^5\,, \tag{8}$$

where $\bar{\alpha}_{\rm s} = N_c\,\alpha_{\rm s}/\pi$, with the number of colors $N_c = 3$. Moreover, for light quarks, $\mathcal{C} = 1.0$, $\bar{r}_0^2 = 1/\Lambda^2_{\rm QCD}$, where one has used $\Lambda_{\rm QCD} = 0.23$. Still, $\omega \equiv 2\psi(1) - 2\psi(1/2) = 4\,\ln 2$ and $\tilde{\omega} = 28\,\xi(3)$. The pomeron intercept is given by $\omega_{\mathbb{P}} = 1 + \bar{\alpha}_{\rm s}\,\omega$. The prescription used here is not unique. For instance, for dipole–dipole collisions, the choice would be $\bar{r} = \min(\boldsymbol{r}_1,\boldsymbol{r}_2)$ and $\bar{r}_0 = \max(\boldsymbol{r}_1,\boldsymbol{r}_2)$, having an impact on the final results.

In Fig. 3 are presented the results using the dipole–dipole cross section of (8), considering the effective radius (I) and taking into account three different values for the pomeron intercept. The QPM contribution was also included. In our further analysis one considers the intermediate value $\omega_{\mathbb{P}} = 1.47$, which is steeper than the results from the saturation model. It should be stressed that further phenomenology can be done, for instance taking the overall normalization, the scale $\bar{r}_0$ and the pomeron intercept $\omega_{\mathbb{P}}$ as free parameters. The differences between the predictions of the saturation model and the BFKL approach are already sizable in the energy interval presented here, with important implications in the future TESLA experiment.

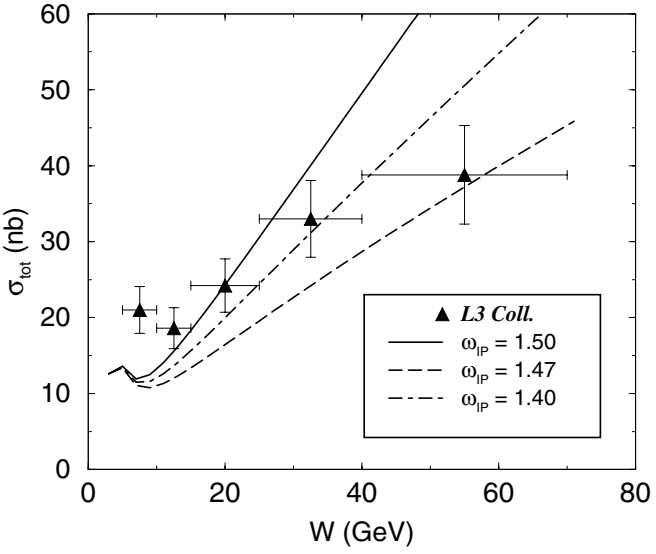

Fig. 3. The cross section for the inclusive charm production in the two-photon process considering the BFKL dipole–dipole approach. The results for three different values for the pomeron intercept $\omega_{\mathbb{P}}$ are presented. The QPM contribution is also included. Data are from the L3 Collaboration

As a final analysis at the photon level, we should calculate the cross section for the interesting final state $2Q\,2\bar{Q}$, which is by definition an onium–onium scattering. In this case the light quarks in the bottom panel of Fig. 1 are replaced by a pair of heavy quarks. The production of this particular configuration was for the first time addressed by Szczurek in [14], calling attention to the fact that the dipole–dipole approach gives a unique prediction of the production of two identical heavy quarks and two identical heavy antiquarks in the final state. The process $\gamma\gamma \to 2Q\,2\bar{Q}$ can only be produced in next-to-leading order calculation in the collinear approach and/or hadronization process. The cross section for this process is given by

$$\sigma^{\rm dd}(\gamma\gamma \to 2Q\,2\bar{Q}) = \int |\Psi_{Q\bar{Q}}(\boldsymbol{r}_1,z_1)|^2\,|\Psi_{Q\bar{Q}}(\boldsymbol{r}_2,z_2)|^2\,\sigma_{\rm dd}\left(\boldsymbol{r}_1,\boldsymbol{r}_2,\tilde{x}_{ab}\right) \times \mathrm{d}^2\boldsymbol{r}_1\,\mathrm{d}^2\boldsymbol{r}_2\,\mathrm{d}z_1\,\mathrm{d}z_2\,. \tag{9}$$

In Fig. 4 are shown the results using (9) and considering the saturation model (radius I and II) and the BFKL dipole–dipole cross section for the charm quark case. In this case, $\bar{r}_0^2 = 1/m_c^2$, and we assume $\mathcal{C} = 1/9$ to reproduce the results in the light quark case. Once again, the

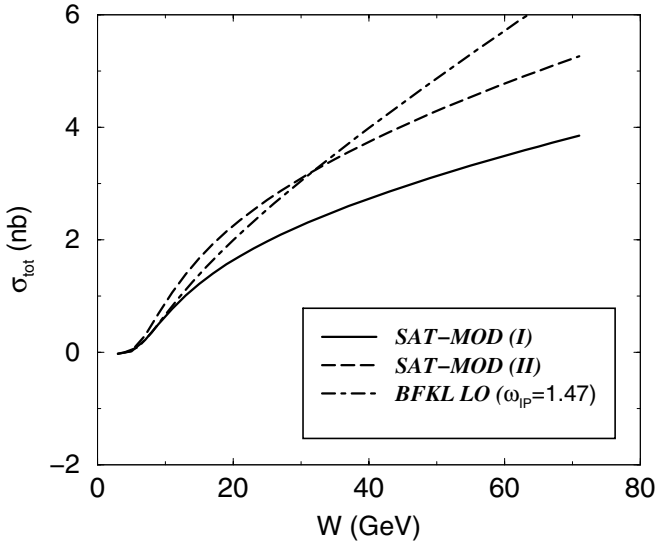

Fig. 4. The cross section $\sigma(\gamma\gamma \to 2c\,2\bar{c})$ considering the saturation model (models I and II) and the BFKL approach, with a pomeron intercept $\omega_{\mathbb{P}} = 1.47$

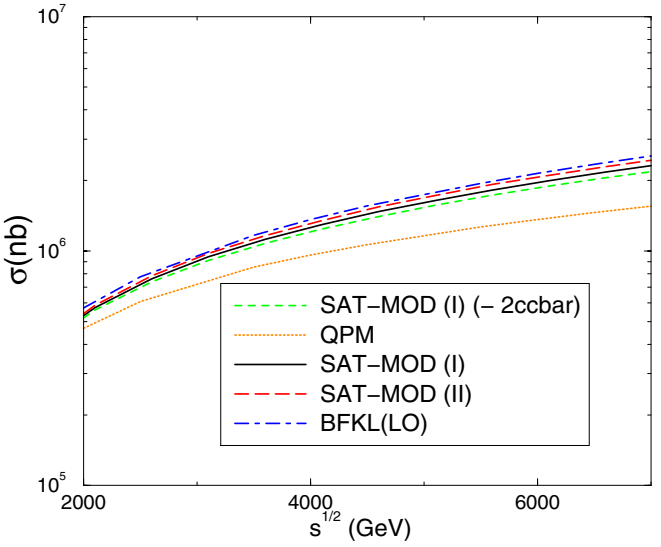

Fig. 5. Inclusive charm pair production in ultraperipheral heavy ion collisions considering the distinct QCD approaches for the $\gamma\gamma$ interaction. For comparison the QPM (*dotted line*) and single $c\bar{c}$ (*dashed line*) cross section are also presented. In the latter case, the contribution of double $c\bar{c}$ production for the inclusive cross section was subtracted

BFKL result is steeper on energy than the dipole model predictions. Similarly to [14], we obtain the result that at high energies the cross section for $2c2\bar{c}$ is about 9% of that for the single $c\bar{c}$ production. It is important to point out the salient fact that in the calculations of the inclusive $c\bar{c}$ production cross section the contribution of this process should be doubled because each of the quarks can potentially be identified experimentally (see the discussion in [14]). In the next section, we present our results for heavy quark production in ultraperipheral heavy ion collisions, considering both contributions for the inclusive heavy quark production cross section.

3 The heavy quark production in ultraperipheral collisions

Having determined the cross sections for heavy quark production at the photon level, in the following the results for ultraperipheral heavy ions collisions will be presented. We emphasize the LHC region, where $W_{\gamma\gamma} \leq 200\,\mathrm{GeV}$, and a luminosity $\mathcal{L} = 4.2 \times 10^{26}\,\mathrm{cm}^{-2}\,\mathrm{s}^{-1}$ for PbPb collisions ($\sqrt{s} = 5500\,\mathrm{GeV}$). Details on the effective two-photon luminosity used here can be found in the previous work in [20]. As referred to above, one has taken $m_c = 1.3\,\mathrm{GeV}$ and $m_b = 4.5\,\mathrm{GeV}$. Further, we discuss the mass dependence of our results.

Our predictions for the inclusive heavy quark cross section and double $c\bar{c}$ pair production at $\sqrt{s} = 5500\,\mathrm{GeV}$ are presented in Table 1. In comparison with the predictions from [29], our results for the inclusive cross section are higher by approximately a factor of 1.8. This enhancement is directly associated to the QCD dynamics, which resums higher order diagrams beyond those considered previously in the literature. It is important to point out the salient fact that this factor is larger than the uncertainty associated with the treatment of the $\gamma\gamma$ luminosity, which is estimated to be about 15% [29]. For RHIC energies (not presented in the table), due to the limited center-of-mass energy of the photon–photon process, the QCD pomeron effects are not important, and our results are similar with those presented in [29].

Table 1. The heavy quark production total cross sections for ultraperipheral heavy ion collisions at LHC ($\sqrt{s} = 5500\,\mathrm{GeV}$) for PbPb

	SAT-MOD (I)	SAT-MOD (II)	LO BFKL
$c\bar{c}$	1 810 000 nb	1 900 000 nb	1 951 200 nb
$b\bar{b}$	2000 nb	–	2200 nb
$2c\,2\bar{c}$	40 000 nb	–	48 000 nb

In Fig. 5 are presented the results for the energy dependence of the inclusive charm pair production in two-photon ultraperipheral heavy ion collisions. The estimates using the saturation model are shown as the solid and long-dashed lines, corresponding to the choice (I) and (II) for the effective radius, respectively. The dipole BFKL calculation is shown in the dot-dashed curve, where we have considered the pomeron intercept $\omega_{\mathbb{P}} = 1.47$. For comparison, the QPM and the single $c\bar{c}$ cross sections are also presented. Despite the deviations between the approaches being large at the photon level, the results for the peripheral reaction are quite similar. This feature is expected, since the two-photon luminosity in nuclear collisions strongly suppresses high energy contributions in comparison with the behavior present in e^+e^- collisions. Concerning the quark mass dependence of our results, we have checked that if one uses $m_c = 1.2\,\mathrm{GeV}$, as done in [29], the cross section grows approximately 25%. There-

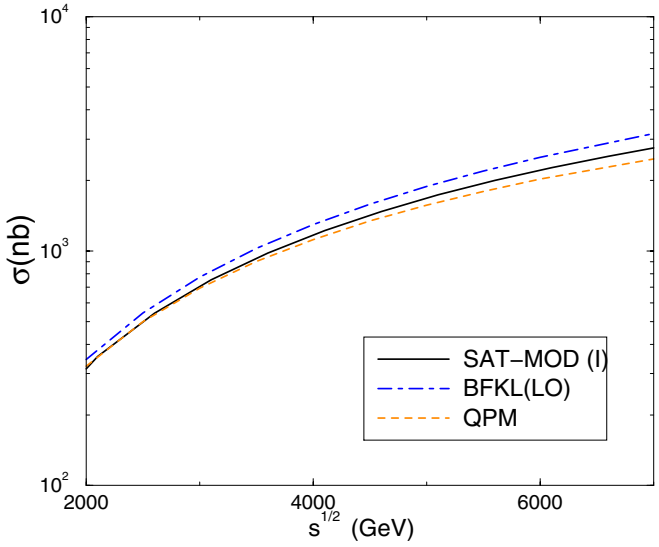

Fig. 6. Inclusive bottom pair production in ultraperipheral heavy ion collisions. For comparison the QPM prediction is also presented

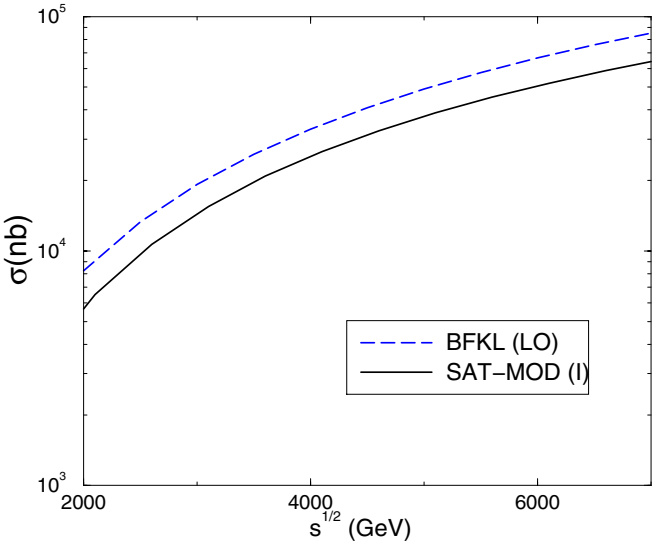

Fig. 7. Double pair charm production in (two-photon) ultraperipheral heavy ion collisions

fore, for this quark mass choice, we predict an enhancement of a factor 2. Here we have used $m_c = 1.3\,\text{GeV}$, since with this choice the experimental data are well described in the dipole approach.

In Fig. 6 are shown the results for the energy dependence of the inclusive bottom pair production in two-photon ultraperipheral heavy ion collisions. The solid line represents the estimate obtained with the saturation approach (model I), the dot-dashed line the dipole BFKL result, and the dashed line is the QPM prediction. The deviation between the saturation and BFKL approaches reaches up to 10%. Similarly to the charm, the analysis of the bottom quark production in ultraperipheral heavy ion collisions would not allow one to discriminate between the distinct kinds of dynamics. However, these effects cannot be disregarded at LHC energies, since our predictions are a factor 2 larger than those obtained in [29].

A comment is in order here. In [29] a detailed analysis of the experimental separation between photoproduction and two-photon interactions was presented. There the authors have estimated that the two-photon cross sections are at least 1000 times smaller than the photoproduction cross section, which makes the experimental separation between the two interactions very hard. Our calculations indicate that the inclusion of the QCD pomeron effects implies higher cross sections at the two-photon level and, consequently, larger cross sections in ultraperipheral collisions. Therefore, the inclusion of these effects implies that the contribution of heavy quark production in two-photon interactions is non-negligible. However, the experimental separation of the two-photon process still remains a challenge.

In Fig. 7 we present separately the results for the double charm pair production in two-photon ultraperipheral heavy ion collisions, obtained from (9). The solid line represents the estimate obtained with the saturation approach (model I) and the dot-dashed line is the dipole BFKL result. The difference between the predictions of the two approaches is about 20% in this particular case. In comparison with inclusive charm pair production, the cross section is two orders of magnitude smaller, but still sizable for an experimental analysis. We stress that the efficiency of flavor tagging is in general very small, which also makes the experimental detection of this process a challenge. However, it is important to emphasize that distinctly from the single pair production which is one background of the photoproduction process, the double heavy quark production can be produced in photo-nucleus reactions only if the multiple interactions are considered. Since, in general, these interactions are suppressed by a factor of about 1000 [37], we find that for this process two-photon interactions and photon–nucleus interactions would be of the same order.

4 Summary

We have investigated the heavy quark production in the ultraperipheral heavy ion collisions from two-photon reactions. The total cross sections at the photon level are calculated using the saturation model, describing the dipole–dipole interaction at high energies including in a suitable way the saturation phenomenon. The dipole BFKL approach is also considered an important test of QCD dynamics, and predictions for the photon–photon cross section using this approach are presented. Both calculations are in reasonable agreement with the current experimental measurements. In particular, we have considered a typical final state allowed by the color dipole picture, namely the double heavy quark pair production $\gamma\gamma \to 2Q\,2\bar{Q}$.

The resulting cross sections in ultraperipheral heavy ion collisions are estimated in these distinct dynamical approaches for the QCD pomeron and presented. Our results

demonstrate that the analysis of the heavy quark production in ultraperipheral heavy ion collisions would not allow one to discriminate between the distinct dynamics. However, the QCD pomeron effects cannot be disregarded at LHC energies, since the cross sections are enhanced by a factor 2 for these effects. Moreover, we have analyzed the double charm pair production and verified that the cross section for this process is sizable, mainly due to the fact that photoproduction background can only be produced by higher order multiple interactions. Our results motivate more detailed studies. In particular, the analysis of the mass and transverse momentum distributions could be useful to discriminate between photon–pomeron and two-photon processes. Work in this direction is in progress.

Acknowledgements. The authors thank S. Klein for valuable suggestions and comments. We are particularly grateful to L. Motyka for his careful reading of the manuscript and for his helpful comments. M.V.T.M. thanks for the support of the High Energy Physics Phenomenology Group (GFPAE, IF-UFRGS) at the Institute of Physics, Porto Alegre. This work was partially financed by the Brazilian funding agencies CNPq and FAPERGS.

References

1. L.N. Lipatov, Sov. J. Nucl. Phys. **23**, 338 (1976); E.A. Kuraev, L.N. Lipatov, V.S. Fadin, JETP **45**, 1999 (1977); I. I. Balitskii, L.N. Lipatov, Sov. J. Nucl. Phys. **28**, 822 (1978)
2. A.H. Mueller, Nucl. Phys. B **415**, 373 (1994)
3. A.H. Mueller, B. Patel, Nucl. Phys. B **425**, 471 (1994)
4. Z. Chen, A.H. Mueller, Nucl. Phys. B **451**, 579 (1995)
5. N.N. Nikolaev, B.G. Zakharov, Phys. Lett. B **332**, 184 (1994); Z. Phys. C **64**, 631 (1994)
6. A. De Roeck, Acta Phys. Pol. B **33**, 2749 (2002)
7. G.P. Salam, Acta Phys. Pol. B **30**, 3679 (1999)
8. K. Golec-Biernat, L. Motyka, A.M. Stasto, Phys. Rev. D **65**, 074037 (2002)
9. K. Golec-Biernat, M. Wusthoff, Phys. Rev. D **59**, 014017 (1999); Phys. Rev. D **60**, 114023 (1999)
10. N. Timneanu, J. Kwiecinski, L. Motyka, Eur. Phys. J. C **23**, 513 (2002)
11. A. Bialas, W. Czyz, W. Florkowski, Eur. Phys. J. C **2**, 683 (1998); J. Kwiecinski, L. Motyka, Eur. Phys. J. C **18**, 343 (2000); N.N. Nikolaev, B.G. Zakharov, V.R. Zoller, JETP **93**, 957 (2001)
12. S.J. Brodsky, F. Hautmann, D.E. Soper, Phys. Rev. D **56**, 6957 (1997); Phys. Rev. Lett. **78**, 803 (1997)
13. M. Boonekamp, A. De Roeck, C. Royon, S. Wallon, Nucl. Phys. B **555**, 540 (1999)
14. A. Szczurek, Eur. Phys. J. C **26**, 183 (2002)
15. A Donnachie, H.G. Dosch, Phys. Rev. D **65**, 014019 (2002)
16. L. Motyka, N. Timneanu, Eur. Phys. J. C **27**, 73 (2003)
17. S.J. Brodsky, V.S. Fadin, V.T. Kim, L.N. Lipatov, G.B. Pivovarov, Pis'ma ZHETF **76**, 306 (2002) [JETP Lett. **76**, 249 (2002)]
18. J. Bartels, A. De Roeck, H. Lotter, Phys. Lett. B **389**, 742 (1996); J. Bartels, C. Ewerz, R. Staritzbichler, Phys. Lett. B **492**, 56 (2000)
19. S.J. Brodsky, V.S. Fadin, V.T. Kim, L.N. Lipatov, G.B. Pivovarov, JETP Lett. **70**, 155 (1999)
20. V.P. Gonçalves, M.V.T. Machado, Eur. Phys. J. C (in press) (2003), [hep-ph/0212178]
21. C.A. Bertulani, G. Baur, Phys. Rep. **163**, 299 (1988)
22. G. Baur, K. Hencken, D. Trautmann, S. Sadovsky, Y. Kharlov, Phys. Rep. **364**, 359 (2002)
23. Ch. Hofmann, G. Soff, A. Schafer, W. Greiner, Phys. Lett. B **262**, 210 (1991)
24. N. Baron, G. Baur, Phys. Rev. C **48**, 1999 (1993)
25. M. Greiner, M. Vidovic, Ch. Hofman, A. Schafer, G. Soff, Phys. Rev. C **51**, 911 (1995)
26. F. Krauss, M. Greiner, G. Soff, Prog. Part. Nucl. Phys. **39**, 503 (1997)
27. F. Gelis, A. Peshier, Nucl. Phys. A **697**, 879 (2002); **707**, 175 (2002)
28. V.P. Gonçalves, C.A. Bertulani, Phys. Rev. C **65**, 054905 (2002)
29. S.R. Klein, J. Nystrand, R. Vogt, Phys. Rev. C **66**, 044906 (2002)
30. M. Vidovic, M. Greiner, G. Soff, J. Phys. G **21**, 545 (1995)
31. N. Baron, G. Baur, Phys. Rev. C **49**, 1127 (1994)
32. M. Klasen, Rev. Mod. Phys. **74**, 1221 (2002)
33. V.M. Budnev, I.F. Ginzburg, G.V. Meledin, V.G. Serbo, Phys. Rep. **15**, 181 (1974)
34. A. Donnachie, H.G. Dosch, M. Rueter, Eur. Phys. J. C **13**, 141 (2000)
35. M. Acciarri et al. [L3 Collaboration], Phys. Lett. B **514**, 19 (2001)
36. E. Iancu, K. Itakura, L. McLerran, Nucl. Phys. A **708**, 327 (2002)
37. S.R. Klein, J. Nystrand, Phys. Rev. C **60**, 014903 (1999)